Physical Behavior of Asphaltenes†

Eric B. Sirota* and Min Y. Lin‡

Corporate Strategic Research, ExxonMobil Research and Engineering Company, Route 22 East, Annandale, New Jersey 08801

Received December 12, 2006. Revised Manuscript Received June 4, 2007

Asphaltenes are molecules which can undergo a thermodynamic liquid−liquid phase separation from sufficiently paraffinic solutions. The asphaltene-rich phase thus formed often has a high glass-transition temperature, and thus a fractal morphology results. Here, we report temperature and time-dependent neutron scattering studies which elucidate the solution behavior of asphaltenes. The temperature−composition dependence of the asphaltene precipitation phase boundary is shown to be consistent with that expected due to solution theory. We report temperature- and concentration-dependent viscosity data which demonstrate that the high viscosity of asphaltene-containing systems is due to their proximity to the glass transition and the reduction of viscosity with dilution is no more than a plasticization effect, or a reduction of the glass transition with dilution.

Introduction

Asphaltenes, often defined by their solubility characteristics are made up of the higher molecular weight and more polar and aromatic molecules in petroleum. We have previously argued that their phase behavior can be explained in terms of the solution behavior of complex molecular mixtures.[1] Furthermore, we have shown that the small-angle "Guinier" scattering in asphaltene-containing mixtures arises from the ephemeral concentration fluctuations characteristic of a multicomponent single-phase solution in the vicinity of phase separation, and divergent "Porod" scattering arises from a second phase of insoluble asphaltenes, or other solids. The scattering peak often observed from concentrated asphaltenes can be considered spinodal decomposition, arrested as a microphase-separated structure. The fractal appearance of precipitated asphaltenes is due to the fact that the phase into which they phase-separate is a highly viscous glasslike liquid state, and the high (and strongly temperature-dependent) viscosity of bitumen and asphaltenic mixtures is due to their proximity to the glass transition.

We have previously discussed at length[1] how data from various techniques including neutron scattering and viscometry have traditionally been interpreted with the *assumption* that one is measuring a colloidal suspension or a micellar system, rather than proving that it is such. While micellar and colloidal models (see refs 2 and 3 and the references in refs 1 and 4) provided simple analogies to explain particular behaviors, by freeing ourselves from taking these analogies too seriously, we have been able to make substantial progress toward understanding the role of asphaltenes in effecting the phase behavior, morphology, and viscosity.

We do, however, point out that these system are not ideal solutions. Strong molecular interactions will exist, allowing molecules to associate. These must be taken into account when applying a solution theory. The association of asphaltenes in dilute solvent solutions has been studied by various techniques[5−7] and is still discussed in terms of colloidal or nanoaggregate pictures. Especially where the system is compositionally highly bimodal, that is, extracted asphaltenes and a light solvent, there can be regimes where such descriptions as colloidal or surfactant analogies can describe some properties. To be clear, asphaltenes do associate. However, they do not behave as surfactants.[8] A hallmark of micellization is the large finite aggregation number, which is in contrast to asphaltene associations which can grow as dimers, trimers, and so forth.

There is one important situation where asphaltenes do indeed exhibit colloidal behavior. After asphaltenes phase-separate from a solution as an extremely viscous, virtually solid or glasslike phase, the particles formed by that phase can act as colloids.[9] As we have discussed previously, however, this colloidal-like asphaltene phase is thermodynamically a liquid (or glass), and at high temperatures or under various compositional situations where the solvent incorporates into that phase, the asphaltene-rich phase will act as a second liquid phase, exhibiting phenomena such as coarsening and coalesecnce rather than colloidal aggregation.[1]

Here, we present neutron scattering studies addressing the temperature and composition dependence of the phase diagram and the kinetics of phase separation. We also present viscosity results showing how the decrease in viscosity with dilution is a plasticization effect. These results help quantify and strengthen the simple understanding of asphaltenes discussed earlier.

* Corresponding author e-mail: Eric.B.Sirota@Exxonmobil.com.

† Presented at the 7th International Conference on Petroleum Phase Behavior and Fouling.

‡ Current address: P.O. Box 3862, Gaithersburg, MD 20885.

(1) Sirota, E. B. *Energy Fuels* **2005**, *19*, 1290.
(2) Pfeiffer, J. P.; Saal, R. N. J. *J. Phys. Colloid Chem.* **1940**, *44*, 139.
(3) Dickie, J. P.; Yen, T. F. *Anal. Chem.* **1967**, *39*, 1847.
(4) Pina, A.; Mougin, P.; Behar, E. *Oil Gas Sci. Technol.* **2006**, *61*, 319.
(5) Andreatta, G.; Bostrom, N.; Mullins, O. C. *Langmuir* **2005**, *21*, 2728.
(6) Sheu, E.; Long, Y.; Hamza, H. In *Asphaltenes, Heavy Oils and Petroleomics*; Mullins, O. C., Sheu, E. Y., Hammami, A., Marshall, A. G., Eds.; Springer: New York, 2007; Chapter 10, pp 259.
(7) Freed, D. E.; Lisitza, N. V.; Sen, P. N.; Song, Y. Q. In *Asphaltenes, Heavy Oils and Petroleomics*; Mullins, O. C., Sheu, E. Y., Hammami, A., Marshall, A. G., Eds.; Springer: New York, 2007; Chapter 11, pp 279.
(8) Friberg, S. E. Micellization. In *Asphaltenes, Heavy Oils and Petroleomics*; Mullins, O. C., Sheu, E. Y., Hammami, A., Marshall, A. G., Eds.; Springer: New York, 2007; Chapter 7, pp 189.
(9) Anisimov, M. A.; Yudin, I. K.; Nikitin, V.; Nikolaenko, G.; Chernoutsan, A.; Toulhoat, H.; Frot, D.; Briolant, Y. *J. Phys. Chem.* **1995**, *99*, 9576.

10.1021/ef060634c CCC: $37.00 © 2007 American Chemical Society
Published on Web 07/26/2007

Experimental Section

Small-angle-neutron scattering (SANS) data were taken on the NG7 30 M diffractometer at the NIST Cold Neutron Research Facility, configured at a wavelength $\lambda = 6.0$ Å and collected using a two-dimensional area detector. The sample-to-detector distance was 2 m for low resolution and 15 m for high resolution. Thus, the overall range of scattering wavevectors studied was $0.002 < q < 0.15$ Å^{-1}. $q = (4\pi/\lambda) \sin \theta$, where 2θ is the scattering angle.

Our deasphalting procedure involved mixing the solvent or solvent mixture at 10 parts solvent to 1 part oil by volume in a round-bottom flask and stirring overnight at room temperature. The mixture containing precipitated asphaltene was then filtered using a preweighed Buchner glass frit (medium) filter. The filter was then washed with the same solvent mixture used for precipitation until the filtrate was clear. The bulk of the solvent was removed from the deasphalted oil using a rotary evaporator at 90 °C for about 1−1.5 h. The deasphalted oil was then further dried by heating in a vacuum oven at 90 °C for 1 h. The solid asphaltenes were dried in a vacuum oven at 90 °C for 14 h and removed from the filter after weighing.

A Canadian bitumen was first subjected to the deasphalting procedure at a toluene/heptane ratio of 30:70. This caused only 1% of the material to be precipitated, about 1/3 of which was inorganic ash. This left the remaining oil and the asphaltenes that would precipitate from it to be "clean". The deasphalted oil from this first step was then subjected to heptane deasphalting, yielding ~15% asphaltenes. These were used in the neutron scattering study presented below.

Neutron Scattering

Much neutron and X-ray scattering work has been done on asphaltenic systems, and references can be found in reviews.[4,10−12] As stated earlier, much experimental data have typically been analyzed and discussed within the context of certain "colloidal" models which we have argued are not representative of the relevant physical phenomena in these systems.[1] Asphaltenes are molecules with moderately high molecular weights and high solubility parameters. Having a high aromatic content, they form true solutions in acceptably aromatic solvents. But due to their molecular weight, the entropy of mixing is not sufficient to keep them in solution if the interaction with the remainder of the solution becomes unfavorable, as occurs, for example, upon the addition of an aliphatic fluid. The phase separation which ensues is thermodynamically a liquid−liquid phase separation which can be understood in the context of the solution theory of molecules. The solidlike character of the asphaltene-rich phase which is thus formed is only due to the fact that the material in the heavier phase is below its glass transition temperature. The solid precipitate has a fractal-like structure since its extremely high viscosity typically does not let it condense into a low-surface-area morphology.

It is well-known that mixtures of species with unfavorable interactions will tend to undergo liquid−liquid phase separation at low enough temperatures. At higher temperatures, the species are not mixed totally randomly but have *dynamically varying compositional inhomogenieties, or concentration fluctuations*. These inhomogenieties give rise to characteristic scattering.[13−15] The local interaction between molecules favor like molecules to find themselves in contact with each other with a preponderance determined by Boltzman-like weighting. Since molecules in a liquid are undergoing constant diffusive motion, such clustering of like molecules is ephemeral. For example, in an "A"/"B" mixture, if one takes a space−time average of the radial distribution function, one finds that the probability of finding an "A" molecule at a given position decreases compared to that of the average composition as you move further away. The distance over which that time−space average probability decays is known as the correlation length, ξ. The correlation length increases as phase separation is approached and diverges continuously at a liquid−liquid critical point. One may be inclined to draw aggregates of dimension ξ in schematic cartoons, but one must always remind oneself that these are not objects with dimension ξ, but rather a statistical description of a liquid. The resulting small-angle scattering arising from such an average distribution is a Lorentzian line shape, which is identical to the Guinier form in the low-angle limit. This scattering is typical of asphaltenes in a single-phase solution.

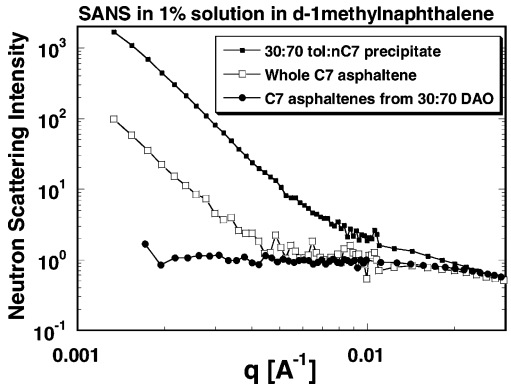

Figure 1. 25 °C SANS patterns of 1% asphaltene solutions in d-1mn of whole nC7 asphaltenes, the 30:70 toluene/heptane asphaltenes, and the C7 asphaltenes obtained from a deasphalted oil of the 30:70 precipitation.

We carried out a SANS study of the temperature dependence and kinetics of asphaltene precipitation. The asphaltenes were dissolved in perdeutero-1-methylnaphthalene (d-1mn), and then perdeutero-dodecane (d-C12) was added. We define β as the weight fraction of d-1mn in the solvent mixture. We define ϕ_{asp} as the asphaltene weight fraction. A magnetic stir bar was contained in a "lollipop-shaped" quartz neutron-scattering cell. This allowed the mixture to be stirred at elevated temperatures to disperse or redisperse the asphaltenes.

There are two important features in the typical neutron-scattering patterns. One is the scattering from local compositional inhomogenieties in the single-phase solution. This can be fit to the Lorentzian form $I(q) \propto 1/[1+(q\xi)^2]$, which approaches a constant finite value at low q values. Approaching the conditions for phase separation, by changing the composition or temperature for instance, the correlation length, ξ, increases. When a second phase appears, Porod scattering results. This is scattering with a q^{-4} power law behavior extending down to very small angles limited by the size of the particles. If the particles are fractal-like, the power will be < 4. In the case of the present data, we are not interested in the details of the fractal morphology, but rather in the existence of the second phase. Thus, in the present analysis, we fixed the power at 4 to get systematic fits for the magnitude of the intensity.

In Figure 1, we show the room-temperature SANS patterns in the low-angle region of 1% solutions in perdeuterated-1-methylnaphthalene of whole nC7 asphaltenes, the solids precipitated using a 30:70 toluene/heptane blend, and the heptane

(10) Sheu, E. Y. *Energy Fuels* **2002**, *16*, 74.
(11) Gawrys, K. L.; Blankenship, G. A.; Kilpatrick, P. K. *Langmuir* **2006**, *22*, 4487.
(12) Mason, T. G.; Lin, M. Y. *J. Chem. Phys.* **2003**, *119*, 565.
(13) Pusey, P. N.; Goldburg, W. I. *Phys. Rev. A* **1971**, *3*, 766.
(14) Zimmermann, H. J.; Wendorff, J. H. *Colloid Polym. Sci.* **1986**, *264*, 292.
(15) Sirota, E. B. *Pet. Sci. Technol.* **1998**, *16*, 415.

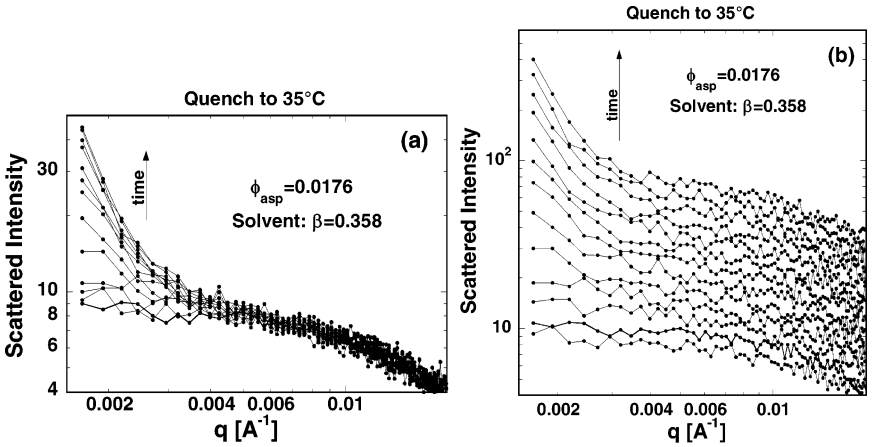

Figure 2. Scattering from $\phi_{asp} = 0.0176$ and $\beta = 0.358$ when quenched to 35 °C and recorded every 10 min. (a) Data superimposed. (b) Offset factors of 1.2.

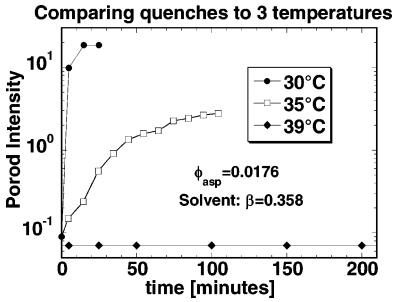

Figure 3. The rise in the Porod intensity showing the kinetics of precipitation on varying temperature for the $\phi_{asp} = 0.0176$ and $\beta = 0.358$ sample.

asphaltenes obtained from the deasphalted oil of the 30:70 precipitation. As can be seen, the low-angle Porod scattering is caused by the material which precipitated with 30:70 toluene/heptane. The material which was precipitated at 30:70 also gave rise to the low-angle scattering at 80 °C (not shown here), telling us that it was not soluble even in 1-methylnaphthalene at elevated temperatures. Analysis of that 30:70 precipitate showed that it was largely inorganic material. Thus, in the rest of the study, we used the cleaned sample (C7 asphaltenes from 30:70 deasphalted oil), which was single-phase when dissolved in 1-methylnaphthalene. An important point here is that one must be careful to distinguish organic second phases from inorganic contaminants which are often not relevant to the problem being studied (i.e., hydrocarbon phase behavior).

In Figure 2, we show the scattering in a solution of $\phi_{asp} = 0.0176$ in a solvent mixture of $\beta = 0.358$ (i.e., 35.8% d-1mn in d-C12) when quenched from a high temperature in the single-phase regime to 35 °C. Data were recorded every 10 min. In Figure 2a, the data are superimposed, showing that there is relatively little change in the scattering from the higher-angle liquid-phase component (since only a fraction of the dissolved asphaltenes comes out of solution at that temperature), while the very-low-angle scattering from the second phase beings to grow in with time. In Figure 2b, each scan is offset by a factor of 1.2.

Fitting the curve to a superposition of a power law and Loretzian, in Figure 3, we show the kinetics of precipitation for three temperatures for the $\phi_{asp} = 0.0176$ and $\beta = 0.358$ sample. At 30 °C, precipitation was very rapid, and at 39 °C, it was barely observable over the time and sensitivity of the experiment. At 35 °C, the second phase grows in over a period of about an hour. Thus, we see the strong temperature dependence of the kinetics of precipitation.

In Figure 4, we show data on a $\phi_{asp} = 0.0176$ and $\beta = 0.358$ solution, at different temperatures in the single-phase regime. In Figure 4a, the scattering data are shown. The temperature ranged from 150 to 50 °C, and the sample was equilibrated at each temperature such that the intensity was no longer changing. As can be seen, the intensity increases with decreasing temperature, and the falloff moves to lower q values (corresponding to larger distances). The data were fit with the Lorentzian form $I = \chi/(1 + \xi^2 q^2)$, yielding the correlation length and the susceptibility which are plotted in Figure 4b. The susceptibility, χ, is a measure of the strength of the fluctuations, or the compositional contrast between the asphaltene-rich regions and the solvent-rich regions. The difference between the correlation length and the susceptibility is illustrated schematically in Figure 5. (We have not quantified the compositional content of these fluctuations; however, this could in fact be done by measuring absolute intensities.)

Looking at the results, we see that, as the temperature is reduced, both χ and ζ increase dramatically with decreasing temperature, χ increasing by a factor of 5 and ζ increasing by a factor of 2. We reiterate that these temperature-driven changes in χ and ζ are equilibrium properties and are thermally reversible. While such scattering is often interpreted by some as measuring the size of basic asphaltene building blocks, it is clear that this is not the case, since they change reversibly with the temperature. We contrast this to the phase transitions and precipitation phenomena as well as redissolution. These are often not as easily reversible. Phase separation requires supersaturation or supercooling to overcome the barriers; redissolution will not have barriers, but the diffusion required to mix two macroscopic phases will take time. These are in contrast to the establishment of compositional fluctuations which occur on much shorter-length scales, as the temperature is varied in a single-phase regime.

In Figure 6, we show, for comparison, data for 1% asphaltene mixtures at room temperature with varying solvent compositions. Here, χ and ζ increase, approaching phase separation compositionally (reducing β). At 20% d-1mn, the mixture was two-phase with precipitated asphaltenes and also resulted in Porod scattering. With some of the asphaltenes out of solution, χ and ζ were lower in the deasphalted liquid phase.

Data for the composition of $\phi_{asp} = 0.01$ and $\beta = 0.325$ are shown in Figure 7. The temperature was decreased in steps from 150 °C to 55 °C, (averaging a rate of 1.0 °C/minute), and then held at 55 °C. Thus, above 60 °C, the sample was in the equilibrium single-phase regime, and any time dependence was

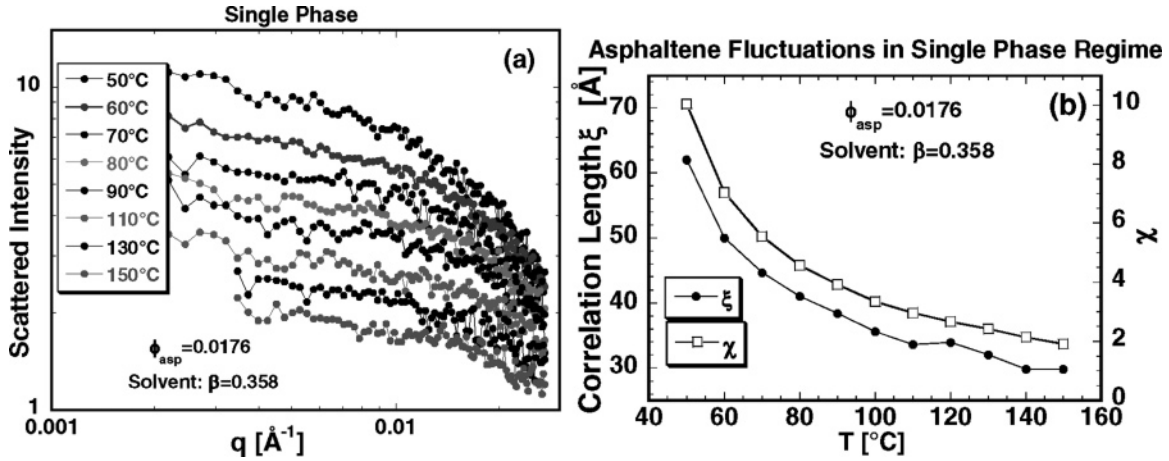

Figure 4. (a) Scattering from the $\phi_{asp} = 0.0176$ and $\beta = 0.358$ sample as a function of the temperature in the single-phase regime. The curves are labeled according to the temperature. (b) The correlation length and susceptibility derived from the curves.

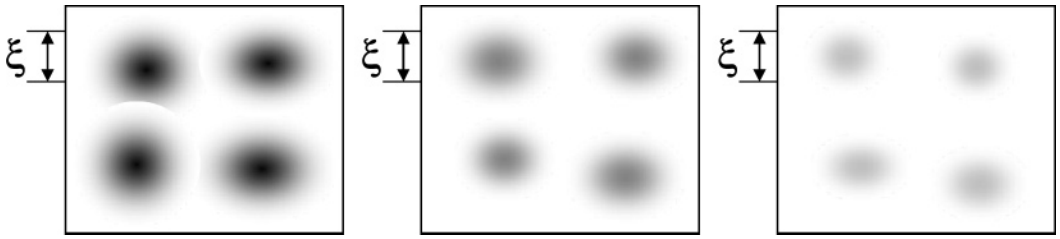

Figure 5. Schematic illustration of the difference between the correlation length and the susceptibility associated with compositional fluctuations. The spatial extent represents the correlation length, and the contrast difference represents the susceptibility.

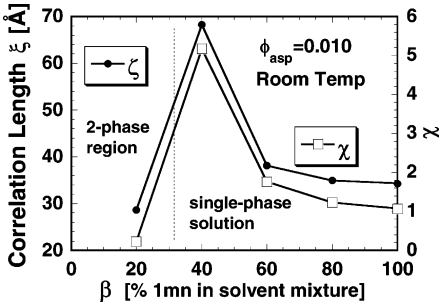

Figure 6. Parameters derived from scattering for $\phi_{asp} = 0.010$ asphaltene mixtures at room temperature with varying solvent compositions. The lines are just guides to the eye. The 20% point is from the liquid phase in a two-phase regime, where the asphaltenes are in a solidlike phase not contributing to this scattering.

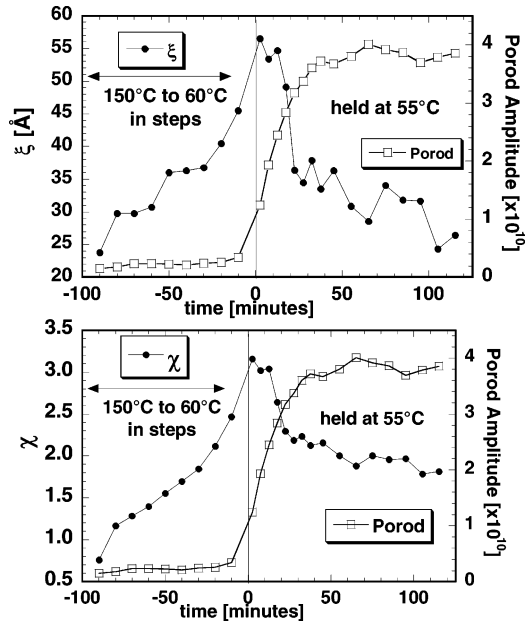

Figure 7. Parameters for $\phi_{asp} = 0.01$ and $\beta = 0.325$ where the temperature was decreased in steps from 150 to 55 °C and then held at 55 °C.

only associated with the thermal equilibration of the sample holder. At 55 °C, phase separation of the asphaltene phase began to occur. This was a process with finite kinetics, which were probed as the sample was repeatedly measured as a function of time, at that temperature.

The data were fit to a superposition of the power law and Lorentzian arising from the phase-separated and dissolved asphaltenes, respectively. The fitted parameters are shown in Figure 7. The Porod scattering is flat above 55 °C and then begins to increase with time when the temperature reached 55 °C and was held there. The finite intensity at the higher temperatures is due to background, which was not easily separable from the data. The fact that this level is independent of the temperature shows that it is not related to the phenomena of interest here.

The correlation length and intensity both increase as the temperature is reduced in the single-phase regime, just as in the previous sample shown in Figure 4b. The lower absolute values of χ can be simply understood in terms of the fact that the sample in Figure 4 has almost twice the asphaltene concentration as the present sample.

It is interesting to note the behavior of χ and ζ at 55 °C as the asphaltene phase separation is occurring. The solution phase is going from an effectively supersaturated state with a large correlation length to one partially depleted in asphaltenes and further from the critical composition. Thus, as asphaltenes leave the solution into a second phase, the scattering from the solution phase changes to reflect this.

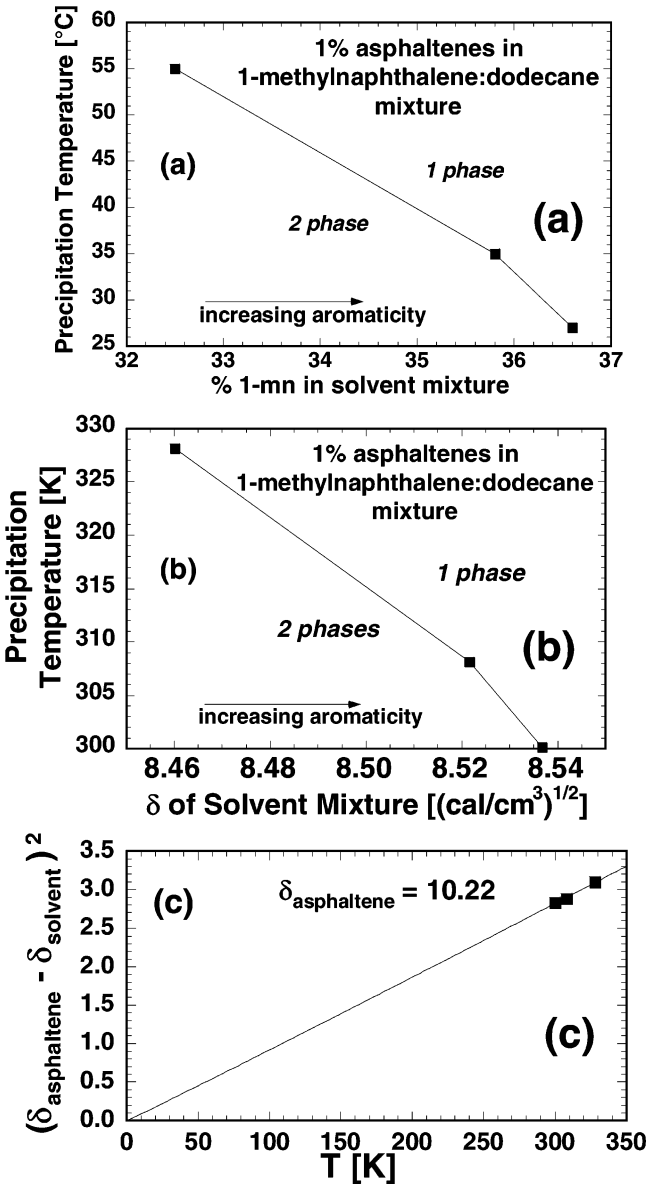

Figure 8. Temperature phase boundaries for 1% asphaltenes in solvent mixtures of varying β, (a) as a function of the composition, (b) as a function of the solubility parameter, and (c) plotted following solution theory (δ^2 in units of cal/cm^3.)

Phase Boundaries

Once precipitated, the asphaltenes will redissolve if the temperature is raised above the phase boundary. Agitation clearly speeds this up, but it is nevertheless a reversible process, with supercooling.

When this system is used, it is insightful to look at the composition dependence of the phase boundaries. We show this in Figure 8a for a 1% asphaltene solution at three different solvent compositions, β. One important point is that the phase boundaries are very sensitive to the composition, varying by ~10 °C for every percent change in β.

Since this solvent pair has a higher boiling point than, for example, heptane/toluene, the large thermal expansion changes that occur approaching the boiling point (more accurately, critical point) will not be significant here. To connect this data with solution theory, we cast the x axis in terms of the solubility parameter of the solvent mixture, δ. Using $\delta_{nC12} = 7.91$ and $\delta_{1methylnaphthalene} = 10.0$ (cal/cm^3)$^{1/2}$ from the literature,[16] we plot the results in Figure 8b in terms of temperature in Kelvin. Since the asphaltene fraction is small and constant, we neglect the asphaltene solubility parameter's contribution to that of the overall mixture here.

In solution theory, temperature only appears in the expression for the Gibbs free energy of mixing, G_{mix}, as $(\delta_i - \delta_j)^2/RT$ (and with the high boiling choice of solvents such that the relative change of the solubility parameters with temperature over this small range can be neglected); the simplest approximation in solution theory is: $T_{precipitation} \propto (\delta_{asphaltene} - \delta_{solvent})^2$.

In Figure 8c, we plot $T_{precipitation} \propto (\delta_{asphaltene} - \delta_{solvent})^2$ versus T, where we have chosen $\delta_{asphaltene}$ to optimize the points to be collinear with each other as well as with the origin. From this, we obtained $\delta_{asphaltene} = 10.22$ (cal/cm^3)$^{1/2}$, which is a very reasonable value based on the aromaticity of the asphaltenes.[16] (These have an atomic H/C ~ 1.15 and MCR ~ 50% and 50% aromatic carbon by ^{13}C NMR.[17])

Viscosity

While, from a true first-principles standpoint, viscosity is far from totally understood, the temperature-dependent viscosity of noncrystallizing fluids follows a modified Arrhenius form:[1] This form, also known as the modified-Vogel−Tammann−

$$\eta = \eta_\infty \exp\{D/[(T/T_0) - 1]\}$$

Fulcher (VTF) equation is not just an empirical fit but is based on theoretical considerations involving entropy change.[18] This form is mathematically equivalent to the Williams−Landel−Ferry (WLF) equation.[19] The WLF equation is cast in terms of and parametrizes the equation using the concept of free volume,[20,21] which can then be related to the glass transition. The modified-VTF equation directly parametrizes the equation in terms of the glass transition, or more specifically the Kauzman temperature.

For crudes, resids, lubes, deasphalted oils, solvents, and their blends, this modified-Arrhenius form well-characterizes the temperature dependence of the viscosity. This is the case for Newtonian single-phase liquids. This form does not include shear thinning behavior that takes place in polymeric systems, or the behavior of multiphase systems such as those with crystallized wax or precipitated asphaltenes. It does apply, however, to situations when the asphaltenes are in solution in a mixture, and with wax dissolved at temperatures above the cloud point.

Simple Arrhenius behavior (thermal activation) $\eta(T) = \eta_\infty \exp(E/kT)$ can describe the temperature dependence of the viscosity only over small temperature ranges. Significant deviations are encountered for non-negligible temperature variations as we showed previously.[1]

The modification of the Arrhenius expression adds one more parameter, which is the finite temperature (T_0) at which the viscosity diverges. This is a manifestation of the glass transition.

(16) Barton, A. M. F. *CRC Handbook of Solubility Parameters and Other Cohesion Parameters*; CRC Press: Boca Raton, FL, 1983.
(17) Wiehe, I. A. *Energy Fuels* **1994**, *8*, 536.
(18) Angell, C. A. *J. Non-Cryst. Solids* **1991**, *131*, 13.
(19) Williams, W. F.; Lande, R. F.; Ferry, J. D. *J. Am. Chem. Soc.* **1955**, *77*, 3701.
(20) King, H. E., Jr.; Segre, P. N.; Appel, M. Viscosity and Diffusion. In *Encyclopedia of Applied Physics V23*; Trigg, G. C., Ed.; Wiley: New York, 1998; Vol. 23.
(21) Grest, G. S.; Cohen, M. H. Liquids, Glasses and the Glass Transition: A Free-Volume Approach. In *Advances in Chemical Physics*; Prigogine, I., Rice, S. A., Eds.; Wiley: New York, 1981; Vol. 48, pp 455.

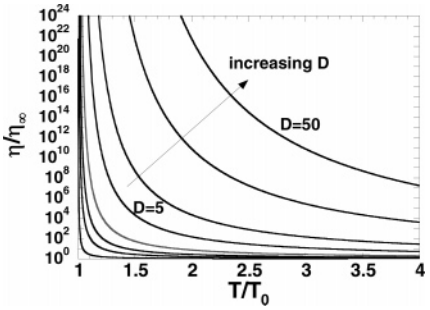

Figure 9. The viscosity versus temperature as parametrized by the Arrhenius expression. The asymptotic value of T_0 and η_∞ are accounted for in the normalized axes. The different curves represent different values of D.

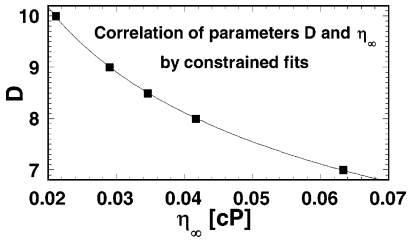

Figure 10. Typical correlation between η_∞ and D in fitting the experimental viscosity versus temperature data.

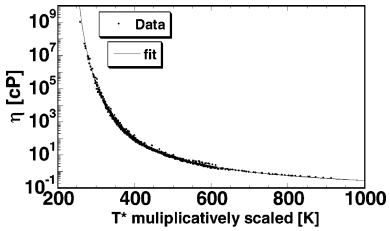

Figure 11. Composite of many viscosity versus temperature data sets of heavy feeds, where each sample's temperature was multiplicatively scaled as to best overlap the rest of the data set.

From a microscopic "free volume" point of view, this represents the fact that the "free volume" goes to zero at a finite temperature. When T_0 approaches 0 K, the simple Arrhenius behavior is recovered. (The glass transition is typically defined as the temperature at which the viscosity reaches 10^{13} Poise, so $T_0 < T_g$.) The parameter "D" is called the "fragility" and can be related to the heat capacity change at the glass transition. (A large D corresponds to small heat capacity jumps at T_g,)[18]

When looking at the parameters in the expression for viscosity, we see that η_∞ is a limiting high-temperature viscosity and can never be actually approached in the temperature ranges of the measurements. Likewise, T_0 is the temperature at which the viscosity exhibits its low-temperature divergence. This limit is also not directly measurable. If we were to know the parameters T_0 and η_∞, then D determines the shape of how the viscosity goes from ∞ at $T = T_0$ to η_∞ at $T = \infty$. This is shown in Figure 9.

Since the actual experimental data are obtained over a relatively narrow range of temperatures as compared to the above plot (to the extent that the data are not exact and have finite experimental uncertainty), the parameters above may not be unambiguously determined but can be correlated in a fit. Thus, we have found that such an experimental $T(\eta)$ curve can usually be reasonably fit with two parameters (for example, T_0 and η_∞), while choosing a range of fixed values for D. In Figure 10, we show a typical correlation between the fitted value of η_∞ and the fixed value of D, chosen in the fit.

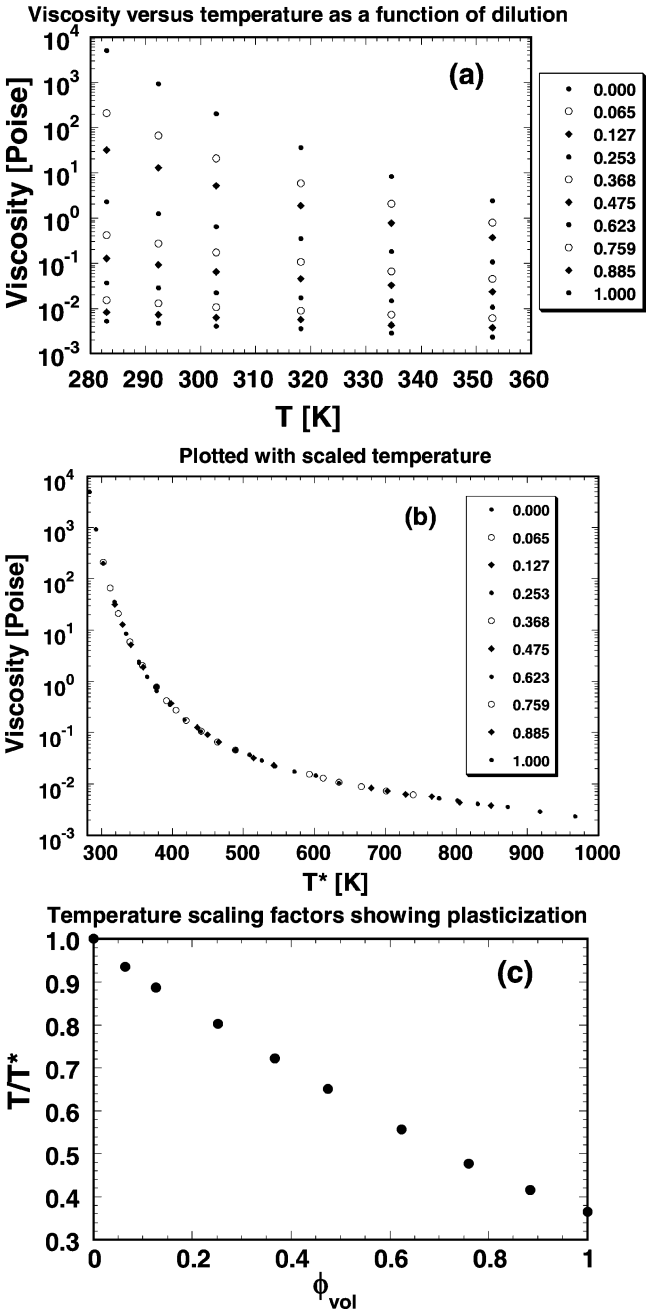

Figure 12. T_0 reduction on the dilution of a 50% C4-asphaltene solution in 1mn, by 1mn. The initial solution was fit to $T_0 = 206$ K. (a) Viscosity as a function of the temperature for varying dilutions.[22] (b) Data with the temperature multiplicatively scaled. (c) The scaling factor giving T/T^*, which gives $T_0/T_{0\text{undiluted}}$ or the reduction of T_0, on dilution. Here, ϕ_{vol} is the volume fraction of the 1mn diluent.

The modified-Arrhenius equation has the interesting property that, if, for a series of materials, D and η_∞ were the same and only T_0 differed between samples, then the $\eta(T)$ curves could be made to overlap by multiplicatively scaling T (in units of K) (the scaling constant being the ratio of the T_0 values between any sample and a reference sample $\eta(T^*)$ where $T^* = \alpha T$.) An important observation is that, for a wide range of mixtures including crude oils, resids, asphaltene solutions, and deasphalted oils, in mixtures and as a series of dilutions, all their temperature-dependent viscosity data could be overlaid simply by applying a multiplicative temperature scaling to each $\eta(T)$ curve. An overall composite of such data is shown below in Figure 11.

Here, the implication is that, while each mixture has its own T_0, their viscosities can be determined using single fixed values for both D and η_∞. η_∞ and/or possibly D are likely to vary throughout such a series of mixtures, and if you look at the data points which are on a log scale covering 11 orders of magnitude in viscosity, it is apparent that substantial errors in the prediction (of over 100%) are still present. What this is telling us is that the many-order-of-magnitude variations in viscosity as a function of temperature and dilution, which occur in heavy crudes, resids, and lubes, can ***mostly*** (although not entirely) be attributed to variation in T_0, or the glass transition temperature.

It is instructive to look at the T_0 as obtained from such fits, as a function of the composition. This is shown below in Figure 12 on data acquired by Redd and Herbolzheimer on a series of asphaltene solutions.[22] (The base solution was C4 asphaltenes from a Canadian bitumen dissolved 1:1 in 1-methylnaphthalene. This was diluted further with 1-methylnaphthalene.) In Figure 12a, the viscosity as a function of the temperature is seen for a series of dilutions of the base solution. In Figure 12b, the temperature is scaled showing that the curves can be overlaid, and in Figure 12c, the T_0 reduction obtained from the scaling constants is plotted as a function of dilution.

The reduction of the glass transition with dilution is thus a "plasticization" effect and is well-known in polymers. While we are far from reaching the actual temperatures of the glass transition, the glass transition shift manifests itself in the viscosity at higher temperatures.

Summary

We have shown that it is important to distinguish second phases arising from hydrocarbon phase separation from those due to insoluble, often inorganic, contaminants. Asphaltenes forming a second phase give distinct scattering from asphaltenes in solution. We demonstrated the strong effect of temperature on the kinetics of asphaltene precipitation and, in the single-phase solution, showed how the correlation length and susceptibility both increase as the temperature is reduced.

The very strong effect of composition on the phase separation temperature, varying by ~10 °C for every percent change in aromatic solvent composition, was also demonstrated. The composition dependence of the asphaltene precipitation phase boundary was shown to be consistent with the expectations of solution theory. A more quantitative treatment of the phase diagram and scattering would require the use of a solution theory well beyond simple mean-field approaches, accounting for the complex molecular structures, distributions and interactions characteristic of asphaltenic systems.

The temperature dependence of the viscosity of single-phase Newtonian fluids follows the modified Arrhenius form. The very strong compositional dependence of the viscosity of asphaltene-containing systems can mostly be accounted for by variations in their glass transition temperatures. Thus, the viscosity reduction upon dilution can be treated as a T_0 reduction, or a "plasticization" phenomena.

By considering asphaltenes in petroleum as molecules in solution, their behavior becomes much more easily explained.

Acknowledgment. We would like to acknowledge discussions with Pawel Peczak, Bernie Silbernagel, Mike Siskin, Howard Freund, Hubert King, and Bill Olmstead. We would also like to thank Eric Herbolzheimer, Dee Redd, Hu Gang, and Jim Sung for the viscosity data and Bob DeLeon for separating the asphaltenes. We acknowledge the support of the National Institute of Standards and Technology, U.S. Department of Commerce, in providing the neutron research facilities used in this work.

EF060634C

(22) Herbolzheimer, E.; Redd, D. unpublished results.